P1.27 INTRASEASONAL AND SYNOPTIC VARIATIONS OF RADIATION BUDGET

Takmeng Wong*
Atmospheric Sciences Research, NASA Langley Research Center
Hampton, Virginia

G. Louis Smith
Virginia Polytechnic Institute and State University
NASA Langley Research Center
Hampton, Virginia

1. Introduction

The Clouds and Earth Radiant Energy System instruments aboard the Terra spacecraft (Wielicki et al., 1996; Barkstrom et al., 2000) have provided measurements of outgoing longwave radiative flux (OLR) and reflected shortwave radiative flux (RSR) over the Earth for more than 2 years. Wong and Smith (2002) used the first year of these data to examine the intraseasonal and synoptic variations of OLR and RSR. This paper presents additional results for these variations.

The time histories of daily OLR and RSR are Fourier-analyzed for each 2.5 degree region of the globe. From these results the temporal spectra are computed for each region for periods of 2 to 364 days. The integral of the spectrum over the complete frequency range is the power of the time history. We denote the integral over a given portion of the frequency range to be the partial power for the range. Maps of partial power show the variability of OLR and RSR over the selected frequency ranges. The ranges of interest correspond to periods of 2 to 60 days. Longer periods are not considered because only 1 year of data are examined.

2. Results

Variations with periods of 20 to 60 days are considered to be intraseasonal and variations with periods of 2 to 20 days are considered to be synoptic. Variations with periods of greater than 60 days are not considered because of the length of record. In order to study intraseasonal variations of longer than 60 days, a record of more than 1 year is required. Figure 1 shows the partial power of OLR in the 20 to 60 day range. The peak centres of spectral power in the 20-60 day range are over a

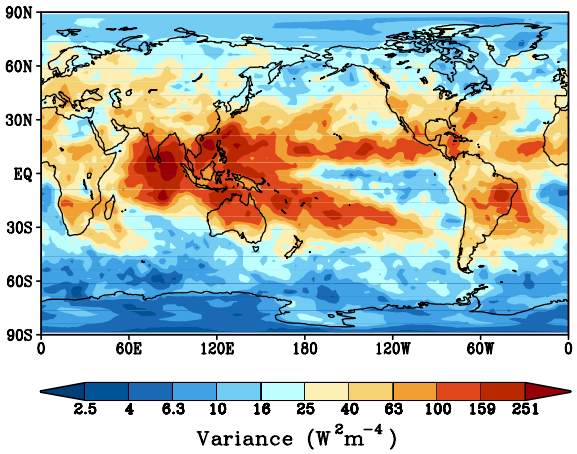

FIG. 1. Regional map of intraseasonal (20 to 60 day range) variability of outgoing longwave radiation.

zone near 15^o North, the Southwest Pacific Convergence Zone (SPCZ), the South American Convergence Zone (SACZ), the Indian Ocean and the South China Sea. The SPCZ vacillates north and south on an intraseasonal time scale. The changing positions of the Intertropical Convergence Zone, including the SPCZ, were noted by Gruber (1972).

Figure 2 is a Hovmueller diagram of OLR showing changes on the Equator during the 1 year period. Eastward propagating waves as low as 160 W-m^{-2} appear against a background of 260 W-m^{-2} or greater. For RSR, the same west-to-east propagating waves appear as 240 W-m^{-2} against a dark ocean back-ground of less than 90 W-m^{-2}. These variations of OLR and RSR are due to high altitude cold clouds associated with the Madden-Julian Oscillation (MJO) in the tropic and do not appear over the subsidence zones of the Pacific and Atlantic Oceans and the eastern part of the Indian Ocean, across which the MJO propagates as a dry wave.

*Corresponding author address: Dr. Takmeng Wong, Mail Stop 420, NASA Langley Research Center, Hampton, Virginia, USA; email address: takmeng.wong@larc.nasa.gov

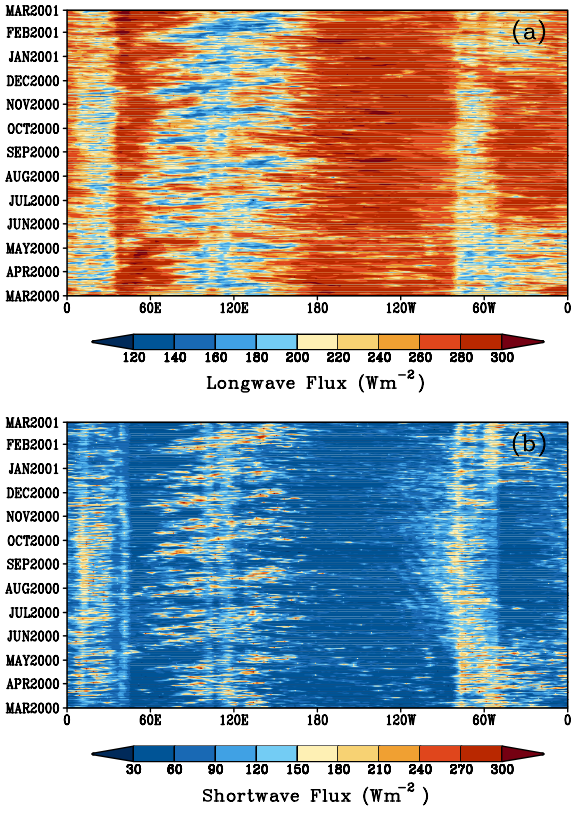

FIG. 2. Hovmueller diagram of (a) OLR and (b) RSR at Equator for 1 year period, showing eastward (west-to-east) propagating wave associated with MJO activities.

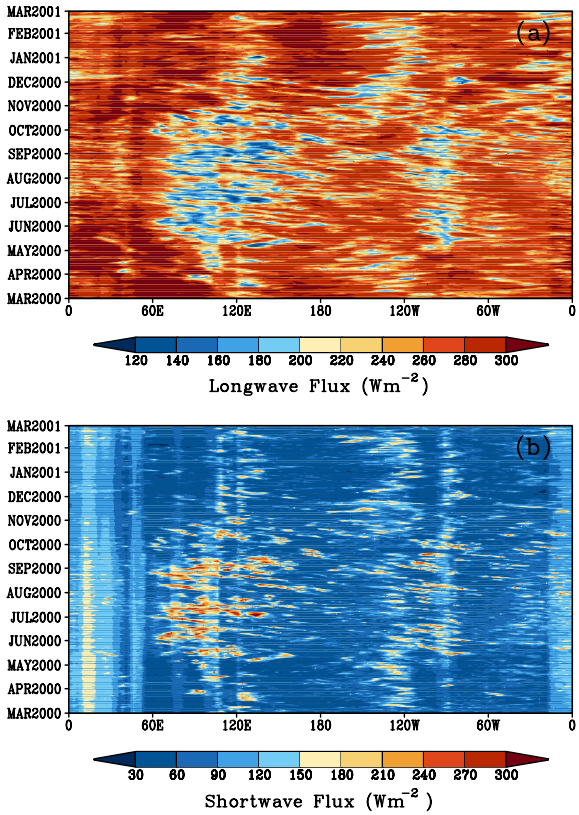

FIG. 3. Hovmueller diagram of (a) OLR and (b) RSR at 15^{o}N for 1 year period, showing westward (east-to-west) propagating waves.

Figure 3a is a Hovmueller diagram of OLR at 15^{o}N and shows waves of 180 W-m^{-2} and less which propagate from east to west across India and Southeast Asia, and the central Pacific Ocean during May to October. From October through April these waves stop their east to west motions. Figure 3b is a similar plot for RSR and shows the same motions with peaks in excess of 240 W-m^{-2} over a background of less than 120 W-m^{-2}. These westward propagating waves require additional research to understand.

Synoptic variations are now examined. Figure 4 is a map of partial power for the 2 to 20 day range for OLR. The ITCZ across the Pacific Ocean, the SPCZ, the SACZ and the Indian Ocean have large values. Next, the mid-latitudes of the Northern Hemisphere and the Roaring 40's of the Southern Hemisphere show considerable activity. There is also a tongue of high variability from China across the Sea of Japan to the Date Line. The spectral density at 2 days has the same pattern shapes. Overall, the geographic patterns of Fig. 4 for the synoptic range are quite similar to those of figure 1 for the intraseasonal range. We conjecture that the intraseasonal variations cascade locally to the shorter period processes. The major difference is the zone near 45^{o}S, where the synoptic power is large but there is little intraseasonal power.

The subsidence zones of the equatorial Pacific Ocean just west of South America, of the Atlantic Ocean between 10^{o} and 20^{o} South and of the eastern Sahara Desert have very little variation at all time scales. OLR and RSR vary mainly due to changes of clouds. Over the eastern Sahara Desert there are few clouds. Over the subsidence regions of the oceans (the Doldrums) there are few clouds except in the boundary layer, where clouds are frequent.

The polar areas show very little variation in the OLR and RSR. However, the polar regions are not regions of little synoptic activity. The small overtones of OLR are due to the OLR being low for both clear and cloudy conditions and the RSR

changes little because the albedo is high for clear or cloudy over the snow and ice.

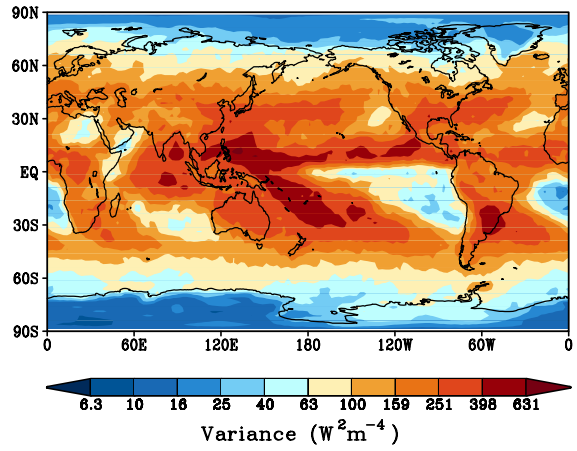

FIG. 4. Regional map of synoptic variations (2 to 20 day range) of outgoing longwave radiation.

The OLR spectral power near the Date Line is shown in Fig. 5, in which the abscissa is the latitude (pole-to-pole) and the ordinate is the spectral power. At 30^{o}S, the spectral power is high for periods out to 5 days at the latitude of the SPCZ and the latitude of the ITZC, just north of the equator. At 30^{o}N the spectral power is high out to 8 days.

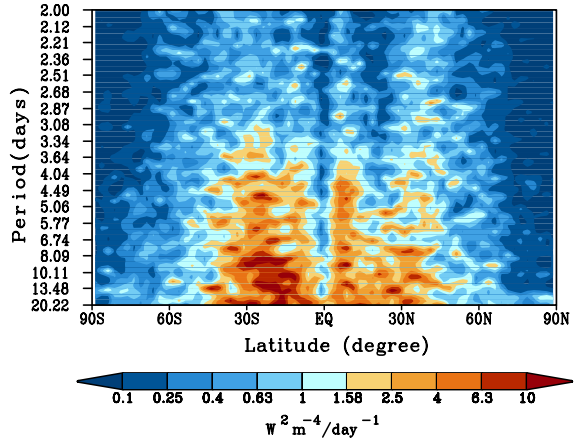

FIG. 5. Spectral power of OLR at 2-20 day range along longitude 183.75 E.

The spectral density is assumed to have a power law distribution for periods of 2 to 20 days (Wong and Smith, 2002) and the exponent is computed for each region. Figure 6 is a map of the exponent for OLR. The exponent has a low value (0.8 or less) in the 45 degree latitude zones over ocean and much higher elsewhere, including subtropical ocean. This low value of the exponent over ocean at mid-latitudes indicates a broad spectrum of OLR, which implies a broad spectrum of processes which create the OLR variations. Stone (1978) demonstrated that the flux of energy must peak near 45^o latitude. Oort (1971) showed that the primary mechanism for transport in this latitude range is transient eddies. These eddies will be accompanied by clouds alternating with clear as baroclinic waves form, advect and decay, resulting in the OLR variations described here.

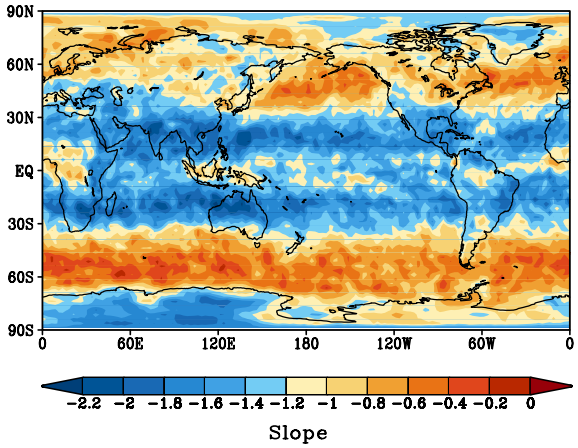

FIG. 6. Regional map of slope of power spectrum in 2 to 20 day range (synoptic) for outgoing longwave radiation.

3. Concluding Remarks

This study raises several questions. What is the nature of the waves propagating from east to west over South Asia and the Eastern Pacific Ocean? How is the temporal spectrum of OLR related to that of other processes? What information can be gained from parameters of the temporal OLR and RSR spectra? Why is the spectrum of OLR in the synoptic range so broad over mid-latitude ocean? Additional studies based on correlated data sets of cloud, atmospheric and surface temperature and moisture, surface albedo and emissivity are needed to answer these questions.

Acknowledgements: This work was supported by the Earth Science Enterprise of NASA through the CERES project at Langley Research Center in Hampton, Virginia. GLS was supported through Langley Research Center by cooperative agreement with Virginia Polytechnic Institute and State

University. CERES/Terra ERBE-like data were provided by the Atmospheric Sciences Data Center of Langley Research Center.

REFERENCES

Barkstrom, B. R., B. A. Wielicki, G. L. Smith, Robert B. Lee, K. J. Priestley, T. P. Charlock and D. P. Kratz, 2000: Validation of CERES/TERRA data, *SPIE 4169, Sensors, Systems and Next-Generation Satellites IV, 17-28*.

Gruber, A., 1972: Fluctuations in the position of the ITCZ in the Atlantic and Pacific Oceans, *J. Atmos. Sci., 29*, 193-197.

Oort, A.H., 1971: The observed annual cycle in the meridional transport of atmospheric energy, *J. Atmos. Sci., 28*, 325-339.

Stone, P.H., 1978: Constraints on dynamical transports of energy on a spherical planet, *Dyn. Atmos. Oceans, 2*, 123-139.

Wielicki, B. A., B. R. Barkstrom, E. F. Harrison, R. B. Lee III, G. L. Smith, and J. E. Cooper, Cloud and the Earth's Radiant Energy System (CERES): an Earth Observing System Experiment, *Bull. Amer. Met. Soc., 77,* 853-868, 1996.

Wielicki, B.A., B. R. Barkstrom, B. A. Baum, T. P. Charlock, R. N. Green, D. P. Kratz, R. B. Lee III, P. Minnis, G. L. Smith, T. Wong, D. F. Young, R. D. Cess, J. A. Coakley Jr., D. H. Crommelynck, L. Donner, R. Kandel, M. D. King, J. Miller, V. Ramanathan, D. A. Randall, L. L. Stowe, and R. M. Welch, "Clouds and the Earth's Radiant Energy System (CERES): algorithm overview," *IEEE Trans. Geosci. and Rem. Sens., 36*, 1127-1141, 1998.

Wong, T. and G. L. Smith, 2002: "Temporal spectra of Earth radiation budget components," *Proc. 16-th Conf. Prob. & Stat. in Atmos. Sci.*, 66-69.